PHYSICAL REVIEW B VOLUME 44, NUMBER 7 15 AUGUST 1991-I

Thermionic emission across $Al_xGa_{1-x}As$ single barriers under hydrostatic pressure

M. Rossmanith and K. Syassen
Max-Planck-Institut für Festkörperforschung, Heisenbergstrasse 1, D-7000 Stuttgart 80, Federal Republic of Germany

E. Böckenhoff
Laboratoire Central de Recherches, Thomson CSF, Domaine de Corbeville, F-91404 Orsay CEDEX, France

K. Ploog and K. von Klitzing
Max-Planck-Institut für Festkörperforschung, Heisenbergstrasse 1, D-7000 Stuttgart 80, Federal Republic of Germany
(Received 25 February 1991)

We have investigated thermally activated transport across GaAs-$Al_xGa_{1-x}As$-GaAs single-barrier heterostructures under hydrostatic pressures up to 6 kbar. The pressure dependence of the activation energy Φ is measured for different mole fractions x in the alloy barrier. For all samples with $X \geq 0.50$, Φ decreases with a pressure coefficient of 17 ± 2 meV kbar^{-1}, indicating the importance of the X valleys in the activated current. However, for a barrier with $x=0.38$, Φ is only observed to decrease above a pressure threshold of 2 kbar, and no decrease is observed at all for a barrier with $x=0.33$. In addition to the pressure dependence of the activation energy, an influence of pressure on the prefactor of the activated current is observed. The results are interpreted in terms of a model that takes into account two different transport channels, one via the Γ point and the other via the X point in the $Al_xGa_{1-x}As$ barrier.

I. INTRODUCTION

In a large variety of electronic devices based on III-V semiconductors, $Al_xGa_{1-x}As$ is used as a barrier for the transport of carriers to the semiconductor layers. For devices that are operated by applying an electric field across a barrier, e.g., field-effect transitors, any current flow across the barrier is undesirable and can degrade the device performance. A similar issue occurs for devices where precise control of the current flow perpendicular to the layers is essential, e.g., resonant tunnel diodes. In this case, charge carriers are thermally activated at room temperature and can surmount the $Al_xGa_{1-x}As$ barrier, again leading to a degradation of the device performance. Hence, finding the most effective barrier for electrons is of great technical importance for the optimization of electronic devices.

In thermionic emission across a single barrier,[1] the ratio of the barrier height Φ and the thermal energy k_BT determines the saturation current density according to the classical Richardson equation

$$J=A^*T^2\exp\left[\frac{-\Phi}{k_BT}\right], \tag{1}$$

where $A^*=em^*k_B^2/2\pi^2\hbar^3$ is called the Richardson constant. Since the band gap of $Al_xGa_{1-x}As$ can be tuned by the AlAs mole fraction x, several experimental studies have been undertaken to examine how the activation energy of thermally activated electrons depends on x.[2–4] This is not trivial because the lowest conduction-band minimum in $Al_xGa_{1-x}As$ for small x is at the Γ point (at the Brillouin-zone center) as in GaAs, whereas for Al-rich $Al_xGa_{1-x}As$ ($x>0.4$), the X minima (at the edge of the Brillouin zone) become the lowest. Studying a series of samples where the $Al_xGa_{1-x}As$ composition is varied systematically is one possible approach to find the most effective barrier for the electrons. However, problems with the interpretation of the data can arise from sample-dependent properties that are not correlated with the different compositions, e.g., the interface quality may vary from sample to sample due to different growth conditions. An alternative method for studying the dependence of electron transport on the barrier height is to apply hydrostatic pressure to a given sample.[5] This avoids the problems arising from the use of different samples. The two methods, however, are not equivalent, because by varying the barrier composition, both the Γ-Γ and the Γ-X conduction-band offsets are changed, whereas hydrostatic pressure changes only the latter. The Γ and X minima have different pressure coefficients and therefore the conduction-band offset between the Γ minimum in GaAs and the X minimum in $Al_xGa_{1-x}As$ can be controlled with pressure. The offset between the Γ minima in the two materials remains essentially unchanged because of the similar pressure coefficients. Hence, high-pressure experiments provide a unique way of monitoring the effect of the Γ-X barrier on electrical transport.

We report here on thermal activation experiments where we combine both methods by applying hydrostatic pressure on $Al_xGa_{1-x}As$ single barriers of different compositions. The measurements were performed in a gas pressure cell permanently connected to a pressure control system allowing a constant pressure to be maintained while increasing the temperature. Only under this condition is the band-edge profile essentially constant during the measurement if we neglect a small temperature dependence of the conduction-band offset, which is an in-

 ©1991 The American Physical Society

herent problem for the interpretation of activation experiments. The experimental data are compared with a quantum-mechanical calculation of the activated current to improve the interpretation. In this calculation the transmission coefficient of the electrons through the barrier plays a crucial role and determines the activation energy and the prefactor of the activated current.

II. SAMPLES AND EXPERIMENTAL SETUP

The samples used in these experiments were grown by molecular-beam epitaxy. A heavily doped GaAs buffer layer was grown on an n^+-type substrate, followed by a 0.5-μm-thick n-type GaAs layer, a 40-nm-thick $Al_xGa_{1-x}As$ barrier, and a 5-nm-thick GaAs spacer. The top electrode is formed by a 1-μm-thick heavily doped GaAs layer. Two samples ($x=0.38,0.62$) have heavily doped GaAs on both sides of the barrier. For each sample the Al content was determined experimentally by reflection high-energy electron diffraction oscillations and by x-ray-diffraction experiments on reference superlattices that were grown just prior to the samples used for this experiment. Both methods provide the exact growth rates needed to determine the thickness of the barrier and its Al content. Samples with dimensions of 5×5 mm^2 were cleaved from all wafers. Mesas between 1.3 and 2.2×10^{-4} cm^2 were produced by standard wet etching techniques. Ohmic contacts were prepared by conventional Au-Ge-Ni metallurgy. The samples were mounted with conducting carbon paste on a sapphire carrier. In order to avoid stress on the sample due to different compressibilities of the sapphire and the sample, only one corner of the sample was glued to the carrier.

For the electrical measurements the sample was mounted in a high-pressure cell that was placed in a bath cryostat and permanently connected to a two-stage gas compressor. We used He gas as a pressure-transmitting medium that does not solidify in the pressure range (0–6 kbar) and temperature range (120–250 K) used in the experiments.[6] The temperature was measured with a Fe-Cu/Ni thermocouple inside the cell. During transport measurements the cell was warmed up from low temperatures at a rate of 20 K per hour while the pressure was kept constant to within ±50 bar. The activated current was measured for different applied voltages between -25 and $+25$ mV with an accuracy of ±100 pA.

The experimental data are evaluated in the conventional manner by plotting $\ln(J/T^2)$ vs $1/T$. The product of the slope and the Boltzmann constant (k_B) is denoted as the "activation energy" Φ, and the ordinate intercept as the "prefactor" A^{**}.

III. MODEL FOR ACTIVATED CURRENT

The quantum-mechanical model for thermal activation starts from the calculation of the current density[7]

$$J=\frac{em_1^*k_BT}{2\pi^2\hbar^3}\int_0^\infty t(E)S(E)dE\ , \tag{2}$$

where $t(E)$ is the transmission coefficient and $S(E)$ the so-called supply function

$$S(E)=\ln\left[\frac{1+\exp(-E/k_BT)}{1+\exp[(-E-eU)/k_BT]}\right]\ , \tag{3}$$

with U being the applied voltage. We assume parabolic bands and separate the motion parallel and perpendicular to the interfaces. The transmission coefficient can then be calculated on one dimension. In the envelope-function approximation, the transmission coefficient is calculated in the usual way by matching the wave function Ψ and its derivative divided by the effective mass $(1/m^*)\nabla\Psi(\nabla=\partial/\partial z)$ at both interfaces.[8] Here m^* stands for the electron effective mass in GaAs (m_1^*) or $Al_xGa_{1-x}As$ (m_2^*). The waves in the contact regions are plane waves,

$$\Psi=e^{ikz}+e^{-ikz}\ . \tag{4}$$

For the wave vector in GaAs we have $k_1=1/\hbar(2m_1^*E)^{1/2}$ with $m_1^*=0.067m_0$. In the barrier region the wave vector is given by $k_2=1/\hbar[2m_2^*(E-V)]^{1/2}$ ($m_2^*=1.1m_0$), where V is the potential step, given either by the conduction-band offset between the Γ minima in GaAs and $Al_xGa_{1-x}As$ (V_Γ) or by the offset between the Γ minimum in GaAs and X minima in $Al_xGa_{1-x}As$ (V_X). It has been shown elsewhere[9] that this model works quite well as long as $V_\Gamma\le V_X$, i.e., as long as the electrical transport occurs via the Γ minima throughout the structure. For large Al concentrations in the barrier when $V_X\le V_\Gamma$, this model overestimates the prefactor of an activated current density, by up to 2 orders of magnitude in the case of pure AlAs. Actually, the continuity condition has to be imposed onto the full Bloch function leading to an interface matrix connecting the envelopes of the wave functions at the interface.[10,11] The interface matrix that will be used here is given by[12]

$$\mathcal{I}_{BA}=\begin{bmatrix}(1-\gamma^2)^{1/2} & -\gamma & 0 & 0\\ \gamma & (1-\gamma^2)^{1/2} & 0 & 0\\ 0 & 0 & (1-\gamma^2)^{1/2} & -\gamma\\ 0 & 0 & \gamma & (1-\gamma^2)^{1/2}\end{bmatrix};\quad \begin{bmatrix}\Psi_\Gamma\\ \Psi_X\\ \nabla\Psi_\Gamma\\ \nabla\Psi_X\end{bmatrix}\ . \tag{5}$$

The base vectors of this matrix are given in square brackets and correspond to the envelope functions for an electron at the Γ point (Ψ_Γ) and at the X point (Ψ_X) and their derivatives ($\nabla\Psi_\Gamma, \nabla\Psi_X$). The off-diagonal matrix elements lead to a mixing among the functions and among their derivatives. Only the parameter γ is necessary to adjust the amount of mixing between the waves. This is similar to the problem treated by Büttiker.[13]

Since the tunneling problem is described by propagating or evanescent waves in positive or negative z directions, the transfer matrix $\mathcal{M}$ through the barrier is written in a different base. The base transformation matrix $\mathcal{T}_b$ connecting the interface and transfer matrices can easily be deduced from

$$\Psi = a_1 e^{+ikz} + a_2 e^{-ikz} , \tag{6}$$

$$m^{*-1}\nabla\Psi = i m^{*-1} k a_1 e^{+ikz} - i m^{*-1} k a_2 e^{-ikz} . \tag{7}$$

At the contact regions a vector consisting of the amplitudes of plane waves traveling in positive and negative z directions can be transformed into a vector consisting of the envelope function and its derivative through

$$\begin{bmatrix} \Psi \\ \nabla\Psi \end{bmatrix} = \begin{bmatrix} 1 & 1 \\ ik/m^* & -ik/m^* \end{bmatrix} \begin{bmatrix} a_1 \\ a_2 \end{bmatrix}; \quad \begin{bmatrix} e^{ikz} \\ e^{-ikz} \end{bmatrix} . \tag{8}$$

The extension to vectors with four components as indicated in Eq. (5) is straightforward and leads to a base transformation matrix

$$\mathcal{T}_b = \begin{bmatrix} 1 & 1 & 0 & 0 \\ 0 & 0 & 1 & 1 \\ ik/m^*_\Gamma & -ik/m^*_\Gamma & 0 & 0 \\ 0 & 0 & ik/m^*_\Gamma & -ik/m^*_\Gamma \end{bmatrix}; \quad \begin{bmatrix} e^{ik_\Gamma z} \\ e^{-ik_\Gamma z} \\ e^{ik_\Gamma z} \\ e^{-ik_\Gamma z} \end{bmatrix} . \tag{9}$$

Hence, the equation for tunneling through the barrier is given by

$$\mathbf{a} = \mathcal{T}'_{BA} \mathcal{M} \mathcal{T}'_{AB} \mathbf{t} , \tag{10}$$

where

$$\mathcal{T}'_{BA} = \mathcal{T}_b^{-1} \mathcal{T}_{BA} \mathcal{T}_b , \tag{11}$$

$$\mathcal{T}'_{AB} = \mathcal{T}_b^{-1} \mathcal{T}_{AB} \mathcal{T}_b , \tag{12}$$

and $\mathbf{a}$ consists of the amplitudes of the incident and reflected waves while $\mathbf{t}$ consists of the amplitudes of the transmitted waves. The first and second components of the equation describe the Γ-Γ-Γ channel and the third and fourth describe the Γ-X-Γ channel.

Now the problem can be formulated as follows. A wave function at the Γ point in GaAs is incident on the barrier. The amplitude of this wave is partially transferred to the X minimum by the interface matrix. The matrix $\mathcal{M}$ transmits two waves through the barrier according to the two different conduction-band offsets and effective masses for the Γ and X channels. In the collecting electrode, far enough behind the second interface, there is again only one propagating wave that has Γ-point symmetry. The vector $\mathbf{t}$ is given by

$$\mathbf{t} = \begin{bmatrix} t_1 \\ 0 \\ t_3 \\ 0 \end{bmatrix}; \quad \begin{bmatrix} e^{ik_\Gamma z} \\ e^{-ik_\Gamma z} \\ e^{ik_\Gamma z} \\ e^{-ik_\Gamma z} \end{bmatrix} , \tag{13}$$

since nothing is reflected back from infinity. The indirect Γ channel is only populated by the interface. Therefore, the amplitude a_3 is set to zero in the emitting contact and $\mathbf{a}$ is given by

$$\mathbf{a} = \begin{bmatrix} a_1 \\ a_2 \\ 0 \\ a_4 \end{bmatrix}; \quad \begin{bmatrix} e^{ik_\Gamma z} \\ e^{-ik_\Gamma z} \\ e^{ik_\Gamma z} \\ e^{-ik_\Gamma z} \end{bmatrix} . \tag{14}$$

The solution of Eq. (10) provides the amplitudes t_1 and t_3 of the transmitted waves and hence the transmission coefficient t.

The following inputs have been used for the quantitative calculation: the dependence of the conduction-band offset between the Γ minimum in GaAs and $Al_xGa_{1-x}As$ is given by[14–16]

$$\Delta E_c^\Gamma = \begin{cases} 0.86x \quad \text{for } 0 \le x \le 0.45 & (15) \\ 0.86x + 1.15(x-0.45)^2 \quad \text{for} 0.45 \le x \le 1. & (16) \end{cases}$$

The conduction-band offset between the Γ minimum in GaAs and the X minimum in $Al_xGa_{1-x}As$ is described by[15]

$$\Delta E_c^X = 0.44 - 0.42x + 0.14x^2 \quad \text{for } 0 \le x \le 1. \tag{17}$$

For the effective electron masses, the conduction-band masses are used because the electrons do not tunnel through thick barriers under the low bias applied in the present experiment. We have used

$$m_2^* = (0.067 + 0.083x) m_0 \tag{18}$$

for the Γ channel and

$$m_2^* = 1.1 m_0 \tag{19}$$

for the X channel.[15] A small pressure dependence of all effective masses[17]

$$m^*(p)/m^*(0) = 1 + 6.15 \times 10^{-3} p(\text{kbar}) - 1.22 \times 10^{-5} p^2(\text{kbar}) \tag{20}$$

is included but has no significant impact on the result. The small compression of the barriers ($<1\%$) has been neglected.

The amount of mixing of the Γ and X waves is con-

trolled by γ in the interface matrix where $\gamma=0$ (1) means that the X (Γ) channel is completely opaque. In the following we shall briefly speak of J_X and J_Γ for the current flowing through the X and Γ channels, respectively.

In summary, this model allows the calculation of the transmission coefficient for coherent waves with an arbitrary amount of mixing. It is assumed in this model that there is no scattering; the wave vector parallel to the interfaces is conserved. Thus only the X minimum longitudinal to the z direction is involved in the transport process.

IV. RESULTS AND DISCUSSION

All samples investigated display the well-known linear behavior of $\ln(J/T^2)$ vs $1/T$ with a constant slope. As an example, the result for $x=1.00$ and $p=4.3$ kbar is shown in Fig. 1. Applying pressure to a sample shifts down the X minimum in $Al_xGa_{1-x}As$ relative to the Γ minimum in GaAs. Since the Γ minima in both materials have similar pressure coefficients that differ only by about 1 meV $kbar^{-1}$ (Refs. 18 and 19), any pressure dependence of the activation energy is closely connected with the variation of the Γ-X barrier. This effect is clearly observed for all samples with $x\geq 0.50$ where the activation energy decreases linearly with a pressure coefficient of -17 ± 2 meV $kbar^{-1}$ [Fig. 2(a)]. This coefficient is larger than the one derived, e.g., from photoluminescence experiments in superlattices (-12.5 meV $kbar^{-1}$).[20] However, in a tunneling experiment through a double barrier resonant tunneling structure[16] with $x=0.4$, the pressure coefficient of the barrier height was determined to be -17 meV $kbar^{-1}$, in agreement with the present result. The origin of this difference between transport and optical data is not yet understood.

An influence of the L minimum on the experimental activation energy can be excluded because the Γ-L conduction-band offset is larger than the Γ-X conduction-band offset. Furthermore, the pressure dependence of the band gap at the L point has a positive sign,[15] making the X minimum even more favorable with increasing pressure.

The pressure dependence of the activation energy for $x=0.38$ exhibits an interesting behavior. Up to a threshold pressure of $p_{th}=2$ kbar the activation energy Φ stays essentially constant. Only beyond p_{th}, Φ decreases with the same slope as for the samples with $x\geq 0.50$. Φ depends sensitively on how the total current J flowing through the sample is composed of J_Γ and J_X. As long as J_Γ dominates, the activation energy will be determined by the conduction-band offset between the Γ minima in GaAs and $Al_xGa_{1-x}As$ (V_Γ). When J_X is dominating, V_X will determine the activation energy, which then becomes pressure dependent. The sample with $x=0.38$ exhibits the crossover between the two different behaviors. For $p\leq 2$ kbar, J_Γ contributes the major part to the activated current density and hence there is no pressure dependence of the activation energy. For $p>2$ kbar, J_X dominates in all samples with $x\geq 0.38$ and they exhibit the same pressure dependence. It is important to note that for $x=0.38$ and at $p=0$, V_X is already smaller than V_Γ. This means that even when the conduction-band

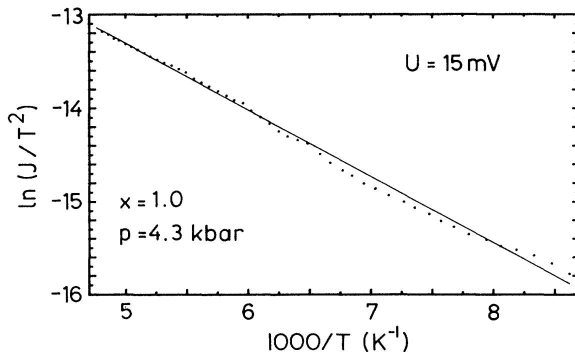

FIG. 1. Plot of $\ln(J/T^2)$ vs $1/T$ for sample with $x=1.00$ under hydrostatic pressure of 4.3 kbar.

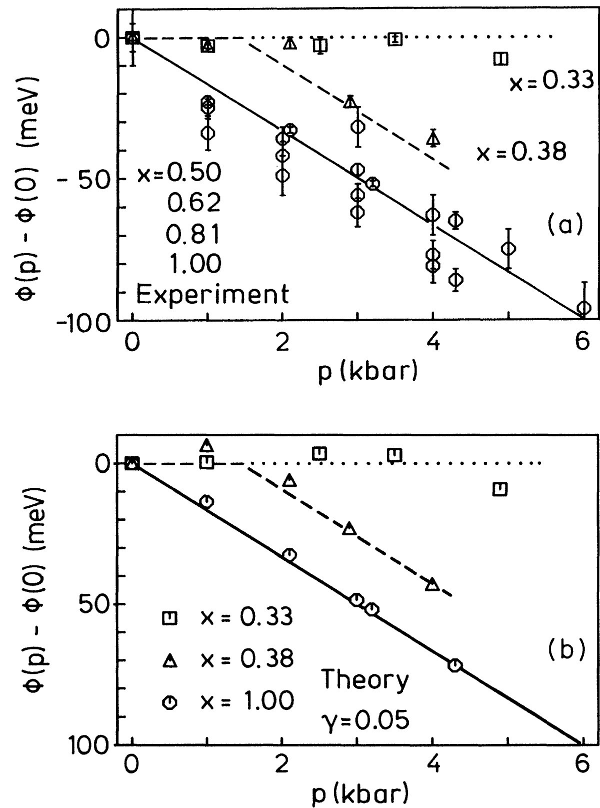

FIG. 2. (a) Difference of the activation energy Φ at finite pressures p and at $p=0$ as a function of p for $x=0.33$, 0.38, 0.50, 0.62, 0.81, and 1.00. (b) Difference of the calculated activation energy Φ at finite pressures p and at $p=0$ as a function of p for $\gamma=0.05$ and an applied voltage of $U=10$ mV for $x=0.33$, 0.38, and 1.00. In (a) and (b) the straight line indicates a pressure coefficient of -17 meV $kbar^{-1}$. The dashed and the dotted lines indicate either 0 or -17meV $kbar^{-1}$.

minima have just crossed, J_Γ remains dominant. This shows that the indirect X channel is less transparent as the direct Γ channel for similar conduction-band offsets. This fact is reflected in the model by $\gamma < 1$ and the larger effective mass for the X electrons.

For the sample with $x = 0.33$, the activation energy is found to be constant for pressures up to $p = 4.9$ kbar. The bands cross at $p = 2$ kbar for this composition. The interpretation of these data is similar to that of the sample with $x = 0.38$, but now the critical pressure p_{th} is above 4.9 kbar.

For a better understanding of the pressure dependence of Φ, simulations are performed by evaluating Eq. (2) in the temperature range where the measurements were performed yielding the temperature-dependent current density $J(T)$. To be close to the experimental situation, the applied voltage was chosen to be $U = 10$ mV. These data are then analyzed in the same way as the experimental ones by a linear fit of $\ln(J/T^2)$ vs $1/T$, providing Φ and A^{**}. The quantitative analysis of the simulations suffers from the uncertainty in the magnitude of γ. For GaAs/AlAs superlattices, a value of 0.04 for γ is found experimentally.[12] From theory, it is clear that γ is closely connected with the band structure of the two materials forming the interface. Hence, γ is expected to depend on the mole fraction x. Furthermore, since hydrostatic pressure also changes the band structure, a pressure dependence of γ cannot be excluded but will be neglected in the following.

In Fig. 3 we show the transmission coefficient $t(E)$. The different effects of the mixing and the pressure on the activated current density $J(T)$ can be demonstrated best on this object. The $x = 0.38$ case was chosen as an example because this composition allows one to observe the crossover from the pressure-independent activation energy to a pressure-dependent one in the pressure regime accessible in the present experiment. Figure 3(a) displays $t(E)$ for $p = 0$ and $\gamma = 0.05$. This choice for γ is justified later. For $E > V_\Gamma$, there are virtual resonances on top of the Γ-point conduction-band profile with maxima $t(E) = 1$. In the range $V_X < E < V_\Gamma$ a series of sharp peaks is visible. They correspond to virtual resonances of the Γ-X-Γ conduction-band profile. In comparison to the resonances for the Γ-Γ-Γ profile, the peak values are reduced by approximately a factor γ^2. This demonstrates that γ governs to a large extent the effectiveness of the indirect X channel. Hydrostatic pressure lowers the indirect potential step V_X. Figure 3(b) shows $t(E)$ for $\gamma = 0.05$ and $p = 2$ kbar and now the virtual resonances start at much lower energies and persist over a larger energy range. Even though $t(E)$ is strongly modulated, the integration of Eq. (2) yields a result for $J(T)$ that can be analyzed in the same way as the experimental data. Figure 4 shows the calculated $\ln(J/T^2)$ vs $1/T$ for $x = 0.38$, $\gamma = 0.05$, and $p = 0$, 2.0, and 2.9 kbar between 125 and 220 K. It is important to note that the Arrhenius plots for $p = 2.0$ and 2.9 kbar are slightly bent. For low temperatures the indirect X channel becomes increasingly important. Therefore, one has to consider the same temperature ranges in experiment and theory when J_Γ and J_X are comparable. However, this type of bending is not

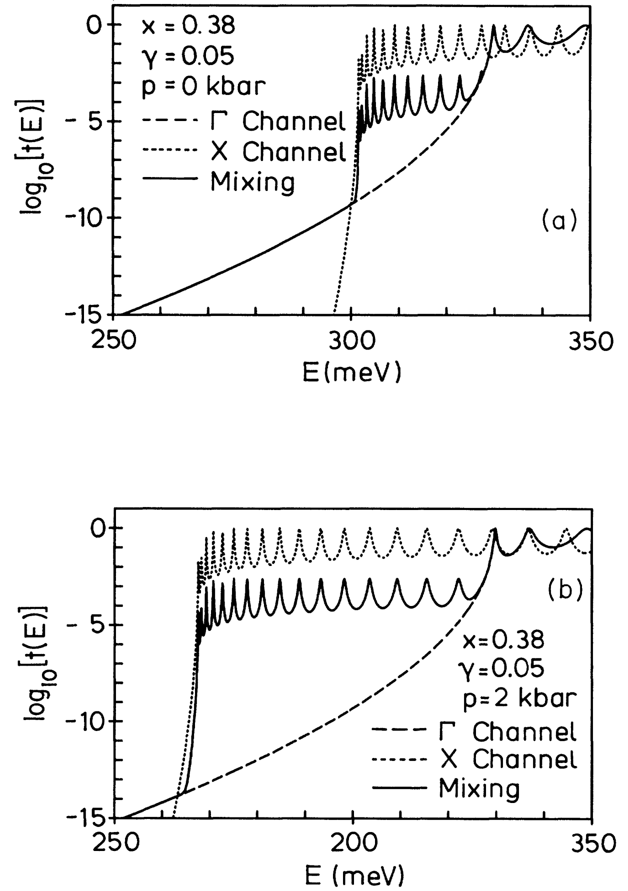

FIG. 3. Transmission coefficient $t(E)$ for $x = 0.38$, $\gamma = 0.05$, and (a) $p = 0$ and (b) $p = 2$ kbar. The dotted lines indicate $t(E)$ in the envelope-function approximation for the Γ and the X channels.

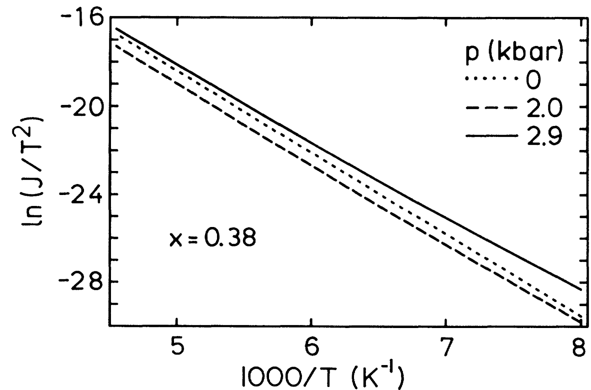

FIG. 4. Activated current density $J(T)$ for $x = 0.38$ and $\gamma = 0.05$ plotted as $\ln(J/T^2)$ vs $1/T$ for $p = 0$ (dotted line), 2 (dashed line), and $p = 2.9$ kbar (solid line).

present in the experimental data. Only for $p=2.9$ kbar is the slope of the activated current density significantly smaller than for $p=0$, although there is a large change in $t(E)$ between $p=0$ and 2 kbar [Figs. 3(a) and 3(b)]. Nevertheless, the activation energy changes only when the indirect current (J_X) becomes comparable to the direct one (J_Γ).

A series of calculations has been performed to fit all data points shown in Fig. 2(a), using γ as a parameter. Intuitively, it is clear that the experimental data for $x=0.33$ set an upper limit for γ because only for a small amount of mixing between the wave functions can a pressure-independent activation energy be expected. On the other hand, the data for $x \geq 0.50$ set a lower limit because only if the mixing is strong enough can one expect a linearly decreasing activation energy. Alone, $x=0.38$ pins down a specific value of γ because there are two distinct regimes of the pressure dependence of Φ, limiting γ to low as well as to high values. Since from an activation experiment it is not possible to determine both the composition and pressure dependence of γ, a single value was calculated for all samples and pressures. As a measure of accordance between experiment and theory, the mean absolute error was used:

$$\Delta\sigma = \left[\frac{1}{N(N-1)} \sum_{i=1}^{N} (\rho_i^{\text{expt}} - \rho_i^{\text{theor}})^2 \right]^{1/2}, \quad (21)$$

with

$$\rho^a = \Phi^a(p) - \Phi^a(0), \quad a = \text{expt, theor} . \quad (22)$$

The total number of experimental data points is $N=33$. Figure 5 shows a plot of $\Delta\sigma$ as a function of γ for $0.01 \leq \gamma \leq 0.18$. It displays a clear minimum in $\Delta\sigma$ for $\gamma = 0.05 \pm 0.01$. The four samples with a linear pressure dependence make $\Delta\sigma$ strongly increasing towards lower values of γ. For $\gamma \geq 0.05$ $\Delta\sigma$ also increases but does so much more weakly, because in this case only a small number of data points of $x=0.33$ and 0.38 are sensitive and hence give a smaller contribution to the total error. Figure 2(b) exhibits the theoretical result of $\Phi(p) - \Phi(0)$ for $\gamma = 0.05$ as a function of pressure. The quantitative and qualitative agreement to experiment supports the presented model. Of course, it would also be possible to choose smaller values for the mixing parameter for those samples with large Al contents, e.g., $\gamma = 0.04$ for AlAs. The experimental prefactors might support this procedure, but their accurate analysis is impeded by the experimental fact that even at pressures of several kbar, variations of ± 50 bar lead to small deviations of the linear behavior of $\ln(J/T^2)$ vs $1/T$ (see Fig. 1).

Extrapolating this model beyond pressures of 6 kbar allows one to estimate the critical pressure of the sample with $x=0.33$. A significant decrease of the activation energy is predicted for pressures between 7 and 8 kbar.

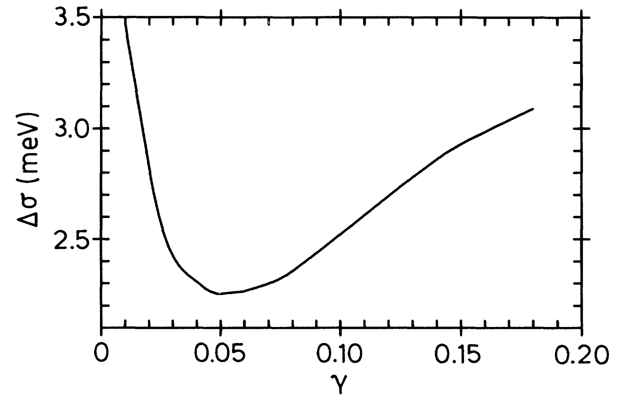

FIG. 5. The mean absolute error $\Delta\sigma$ of $\Phi(p) - \Phi(0)$ between experiment and theory as a function of the mixing parameter γ and the Γ and X channels.

V. CONCLUSION

Thermally activated transport in GaAs-$Al_xGa_{1-x}As$-GaAs single-barrier heterostructures of different compositions has been studied under hydrostatic pressure. A linear decrease of the activation energy is observed with a pressure coefficient of 17 ± 2 meV kbar^{-1} for the Al-rich samples. This coefficient is larger than the one derived from photoluminescence experiments but agrees with other transport measurements. The crossover from a pressure-independent activation energy to a pressure-dependent one is clearly observed for the samples with low Al concentration. The critical pressure where this crossover occurs depends on the Al concentration in the barrier.

Quantum-mechanical calculations assuming that the mixing between Γ and X electron wave functions is 5% are able to simulate the experimental findings. The most important of these is that the X minima must be sufficiently below the Γ minimum so that the current J_X through the indirect X channel is of the same order of magnitude as the current J_Γ through the direct Γ channel. Only then does the pressure dependence of the X minima manifest itself in the electrical transport properties.

ACKNOWLEDGMENTS

The authors would like to acknowledge many helpful discussions with P.A. Schulz, S. Bending, N. Pulsford, and J. Leo, who also provided a part of the computer program. We also want to thank W. Böhringer for his expert technical assistance in running the high-pressure equipment and F. Schartner and I. Jungbauer for bonding and processing the samples.

[1] S. M. Sze, *Physics of Semiconductor Devices* (Wiley, New York, 1981).
[2] P. M. Solomon, S. L. Wright, and C. Lanza, Superlatt. Microstruct. **2**, 521 (1986).
[3] I. Hase, K. Kaneko, and N. Watanabe, J. Appl. Phys. **59**, 3792 (1986).
[4] K. Maezawa, T. Mizutani, and F. Yanagawa, Jpn. J. Appl. Phys. **7**, 1557 (1986).

[5]R. Pritchard, P. C. Klipstein, N. R. Kelly, J. S. Roberts, P. Mistry, B. Soyla, and W. M. Stobbs, Semicond. Sci. Technol. **4**, 754 (1989).

[6]W. F. Sherman and A. A. Stadtmuller, *Experimental Techniques in High Pressure Research* (Wiley, New York, 1987), p. 132.

[7]C. B. Duke, *Tunneling in Solids* (Academic, New York, 1965).

[8]See, for example, D. J. BenDaniel, and C. B. Duke, Phys. Rev. **152**, 683 (1966).

[9]M. Rossmanith, J. Leo, and K. von Klitzing, J. Appl. Phys. **69**, 3641 (1991).

[10]H. Akera, S. Wakahara, and T. Ando, Surf. Sci. **196**, 694 (1988).

[11]T. Ando, S. Wakahara, and H. Akera, Phys. Rev. B **40**, 11 609 (1989); **40**, 11 619 (1989).

[12]N. J. Pulsford, R. J. Nicholas, P. Dawson, K. J. Moore, G. Duggan, and C. T. B. Foxon, Phys. Rev. Lett. **63**, 2284 (1989).

[13]M. Büttiker, Phys. Rev. B **33**, 3020 (1986).

[14]M. Rossmanith, J. Leo, and K. von Klitzing, in *20th International Conference on the Physics of Semiconductors, Thessaloniki, Greece, August, 1990,* edited by E. M. Anastassakis, and J. D. Joannopoulos (World Scientific, Singapore, 1991), p. 1142.

[15]S. Adachi, J. Appl. Phys. **58**, R1 (1985).

[16]E. E. Mendez, E. Calleja, and W. I. Wang, Phys. Rev. B **34**, 6026 (1986).

[17]Z. Wasilewski and R. A. Stradling, Semicond. Sci. Technol. **1**, 264 (1986).

[18]J. D. Lambkin, A. R. Adams, D. J. Dunstan, F. Dawson, and C. T. Foxon, Phys. Rev. B **39**, 5546 (1989).

[19]U. Venkateswaran, M. Chandrasekhar, H. R. Chandrasekhar, B. A. Vojak, F. A. Chambers, and J. M. Meese, Superlatt. Microstruct. **3**, 217 (1987).

[20]M. Holtz, R. Cingolani, K. Reimann, R. Muralidharan, K. Syassen, and K. Ploog, Phys. Rev. B **41**, 3641 (1990).